Journal of Biotechnology 262 (2017) 28–39

Contents lists available at ScienceDirect

Journal of Biotechnology

journal homepage: www.elsevier.com/locate/jbiotec

Research paper

Tridimensional configurations of human mesenchymal stem/stromal cells to enhance cell paracrine potential towards wound healing processes

Marta H.G. Costa[a,b], Todd C. McDevitt[b,c,d], Joaquim M.S. Cabral[a,e], Cláudia L. da Silva[a,e], Frederico Castelo Ferreira[a,e,*]

[a] Department of Bioengineering and IBB-Institute for Bioengineering and Biosciences, Instituto Superior Técnico, Universidade de Lisboa, Lisboa, Portugal
[b] The Wallace H. Coulter Department of Biomedical Engineering, Georgia Institute of Technology/Emory University, Atlanta, GA, USA
[c] Gladstone Institute of Cardiovascular Disease, San Francisco, CA, USA
[d] Department of Bioengineering & Therapeutic Sciences, University of California, San Francisco, USA
[e] The Discoveries Centre for Regenerative and Precision Medicine, Lisbon Campus, Instituto Superior Técnico, Universidade de Lisboa, Av. Rovisco Pais, 1049-001 Lisboa, Portugal

ARTICLE INFO

Keywords:
Encapsulation
Mesenchymal stem/stromal cells (MSC)
Paracrine activity
Spheroids
Wound healing

ABSTRACT

This study proposes to use alginate encapsulation as a strategy to assess the paracrine activity of 3D- and 2D-cultured human bone marrow mesenchymal stem/stromal cells (BM MSC) in the setting of wound repair and regeneration processes. A side-by-side comparison of MSC culture in three different 3D configurations (spheroids, encapsulated spheroids and encapsulated single cells) *versus* 2D monolayer cell culture is presented. The results reveal enhanced resistance to oxidative stress and paracrine potential of 3D spheroid-organized BM MSC. MSC spheroids (148 ± 2 μm diameter) encapsulated in alginate microbeads evidence increased angiogenic and chemotactic potential relatively to encapsulated single cells, as supported by higher secreted levels of angiogenic factors and by functional assays showing the capability of encapsulated MSC to promote formation of tubelike structures and migration of fibroblasts into a wounded area. In addition, a higher expression of the anti-inflammatory factor tumor necrosis factor alpha-induced protein 6 (TSG-6) was demonstrated by RT-PCR for encapsulated and non-encapsulated spheroids. Culture of spheroids within an alginate matrix maintains low aggregation levels below 5% and favors resistance to oxidative stress. These are important factors towards the establishment of more standardized and controlled systems, crucial to explore the paracrine effects of 3D-cultured MSC in therapeutic settings.

1. Introduction

Wound healing is a complex process mediated by several cytokines involved in inflammatory responses and tissue remodeling. The paracrine activity of mesenchymal stem/stromal cells (MSC) can stimulate tissue regeneration, namely promoting proangiogenic, immunomodulatory, antifibrotic and antioxidant cell activity (Caplan and Dennis, 2006). Several MSC-secreted bioactive factors have been suggested to be integrated in signaling networks that mediate wound healing response. Such factors include vascular endothelial growth factor (VEGF), interleukin-6 (IL-6) and hepatocyte growth factor (HGF), known for their role on angiogenesis (Ding et al., 2003; Ferrara, 2001; Gerritsen, 2005; Kwon et al., 2014); stem cell-derived factor-1α (SDF-1α, also known as CXCL12), a chemotactic factor involved in cellular migration (Liu et al., 2012); tumor necrosis factor alpha-induced protein 6 (TSG-6), an important cytokine for the regulation of immunomodulatory processes (Lee et al., 2014), similarly to HGF and IL-6 (Di Nicola et al., 2002; Janssens et al., 2015), which are involved in inflammatory responses (in addition to their role on angiogenesis).

Although the potential benefits of MSC trophic activity have been well described, lack of MSC retention in targeted tissues decreases their impact once delivered *in vivo*. Typical ischemic wounded tissues present high levels of local reactive oxygen species (ROS), such as hydrogen peroxide (H_2O_2), severe hypoxia and inflammation, which dramatically decrease cell viability in wounded sites (Khanna et al., 2010; Potier et al., 2007; Song et al., 2010). In response to the alarm signals triggered in a wounded area, MSC secrete a series of trophic factors involved in the wound healing process. A hypoxic environment, for instance, characteristic of ischemic wounds, leads to activation of hypoxia-inducible factor-1α (HIF-1α), promoting angiogenesis (namely through secretion of VEGF, fibroblast growth factor-2 (FGF-2), HGF, insulin-like growth factor-1 (IGF-1) and thymosin beta-4 (Gnecchi,

* Corresponding author at: Department of Bioengineering and IBB-Institute for Bioengineering and Biosciences, Instituto Superior Técnico, Universidade de Lisboa, Lisboa, Portugal.
E-mail address: frederico.ferreira@tecnico.ulisboa.pt (F.C. Ferreira).

http://dx.doi.org/10.1016/j.jbiotec.2017.09.020
Received 6 June 2017; Received in revised form 27 September 2017; Accepted 27 September 2017
Available online 28 September 2017
0168-1656/

2006)) and inducing migration of fibroblasts and keratinocytes (Tandara and Mustoe, 2004). Particularly, when cultured as 3D spheroids, MSC evidence increased survival in ischemic tissues, while simultaneously present a higher expression of anti-inflammatory and proangiogenic factors with a key role on wound healing mechanisms (Bhang et al., 2011). In a pro-inflammatory environment, MSC were also shown to alter their secretome, in complex feedback mechanisms with surrounding immune cells (Yagi et al., 2010). A stress response, namely through a caspase-dependent mechanism, is thought to be involved on the spheroids upregulated expression of anti-inflammatory cytokines, such as TSG-6, prostaglandin E2 and stanniocalcin-1 (Bartosh et al., 2013; Tsai et al., 2015; Zimmermann and Mcdevitt, 2014). Human bone marrow (hBM) MSC could contribute to restore the oxygen levels and function of wounded tissues through their capability to promote angiogenesis, regulate inflammation and recruit native cells involved in the wound healing process, particularly when organized as spheroids. Nevertheless, the benefits associated with this 3D cell culture might be lost when cells are delivered *in vivo* into the target tissue, as cells tend to migrate from the spheroid to the surrounding extracellular matrix (ECM) as it has been observed in both *in vitro* (Blacher et al., 2014) and *in vivo* settings (Bhang et al., 2012).

To potentiate the response of MSC in regenerative processes, it is crucial to maximize cell survival, retention and function at the injured site. In an oxidative stress environment, matrices such as a pullulan-collagen hydrogel could improve MSC delivery, quenching ROS within ischemic wounds (Wong et al., 2011), an ability that has also been attributed to alginate hydrogels (Eftekharzadeh et al., 2010; Matyash et al., 2012). Encapsulation of BM MSC within a biocompatible and inert biomaterial, such as alginate microbeads, able to mediate cellular paracrine activity can be exploited as a MSC delivery system to study and modulate 3D cellular configurations towards improved wound healing processes. Alginate is an inert, European Medicines Agency (EMA)- and Food and Drug Administration (FDA)-approved material that has been used as a wound healing dressing and cell carrier (Hashimoto et al., 2004; Lee et al., 2010). This polysaccharide can be easily crosslinked with divalent cations (such as Ca^{2+}), resulting in formation of a hydrogel that allows diffusion of growth factors and nutrients/metabolites while simultaneously excludes host immune cells (Strand et al., 2002). Previous studies showed that alginate microcapsules can maintain their integrity for several months once implanted in mice (Landázuri et al., 2012; Safley et al., 2008), therefore retaining cells whose secretome can favor biological processes that take days to months, such as vascularization and tissue repair (Broughton et al., 2006).

Different studies have been exploring differences in the wound healing potential of cell culture performed in 2D monolayer configurations in comparison to 3D-organized cells seeded on gelatin microbeads (Zhao et al., 2015a,b), encapsulated in hydrogel microcapsules (Bussche et al., 2015), aggregated in spheroids cultured under static (Santos et al., 2015) or bioreactor platforms (Kwon et al., 2015). Nonetheless, our study presents, at the best of our knowledge, the first side-by-side comparison of the paracrine potential of BM MSC cultured in three different 3D configurations (spheroids, encapsulated spheroids and encapsulated single cells) against monolayer culture, focusing wound healing and angiogenesis. Functional assays aiming to unravel several aspects of wound healing, including the chemotactic, wound closure and angiogenic potential of MSC were performed. The advantages of a 3D cell culture of non-encapsulated MSC spheroids were assessed, particularly regarding their protection against an oxidative stress environment and compared with the most conventional 2D culture of MSC grown as monolayer adherent cells to tissue culture polystyrene (TCPS). Importantly, the use of alginate to promote encapsulation of either single MSC or 3D-organized MSC spheroids (Fig. 1) facilitated a direct comparative approach to assess the enhanced trophic properties of 3D spheroids over single-cultured MSC. This could therefore favor a more straight evaluation of the role played by cellular aggregation on the paracrine potential of MSC, not limiting the study to comparison with TCPS-adherent cells, and further allowing us to evaluate the advantages of using biomaterial vehicles to culture MSC spheroids.

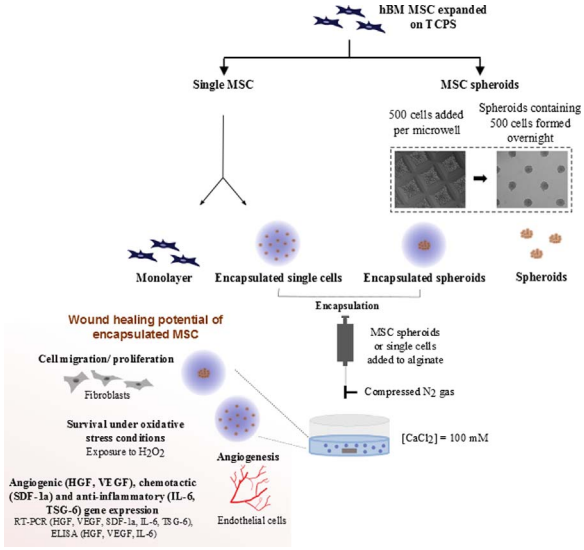

Fig. 1. Schematic representation of the experimental setup. BM MSC were expanded on TCPS and cultured as monolayer adherent cells, encapsulated single cells, non-encapsulated spheroids or encapsulated spheroids. Spheroids incorporating 500 cells were formed overnight in microwells and either cultured as non-encapsulated cells or encapsulated in alginate. Both spheroids and single MSC were embedded in alginate and extruded through a syringe needle into a calcium bath. The wound healing potential of encapsulated spheroids, encapsulated single cells, non-encapsulated spheroids and monolayer adherent MSC was studied through evaluation of survival under oxidative stress conditions, expression of relevant genes for the wound healing response, assessment of their angiogenic potential and involvement on the migration/proliferation of surrounding cells.

2. Materials & methods

2.1. Cell culture

hBM MSC (from at least 3 different individual donors, passage 4–6), isolated and immunophenotypically characterized as previously described (dos Santos et al., 2010), were cultured in low-glucose Dulbecco's Modified Eagle Medium (DMEM) supplemented with 10% (v/v) fetal bovine serum (FBS) (MSC qualified), 1% Antibiotic-Antimycotic (A/A) (all from Life Technologies). Cells were seeded at a density of 2–3 × 10^3 cells/cm^2 on 75 cm^2 Falcon® T-flasks in 10 mL of medium, which was exchanged every three to four days. After reaching approximately 70% confluence, cells were harvested with 0.05% (w/v) trypsin (Life Technologies) − 1 mM Ethylenediaminetetraacetic acid solution (EDTA) (Sigma). MSC were then cultured as monolayer cells, encapsulated as single cells or used to preform spheroids, which were cultured either as non-encapsulated or alginate-encapsulated spheroids for 7 days (Fig. 1). Non-encapsulated spheroids were cultured in suspension on a rotary orbital shaker (Rotamax 120, Heidolph) at 65 rpm whereas encapsulated single cells and encapsulated spheroids (all added at a ratio of 5 × 10^4 cells/mL of expansion medium) and monolayer cells (plated at an initial density of 3 × 10^3 cells/cm^2) were cultured under static conditions in Falcon® 6-well plates. Non-encapsulated spheroids were cultured on Ultra-Low Attachment plates (Corning) and culture medium was changed at day 4 of culture.

2.2. Formation of spheroids and spheroid size measurement

MSC spheroids with 500 cells per spheroid were formed overnight in an array of agarose (SeaKem® LE Agarose) 400 × 400 μm-sized

Table 1
Taqman primers for RT-PCR.

Gene symbol	Gene name	Role	Assay ID
GAPDH	Glyceraldehyde-3-phosphate dehydrogenase	Endogenous control	Hs02758991_g1
CXCL12	Chemokine (C-X-C motif) ligand-12	Chemotaxis	Hs03676656_mH
HGF	Hepatocyte growth factor	Angiogenesis; immunomodulation	Hs00300159_m1
IL-6	Interleukin-6	Angiogenesis; immunomodulation	Hs00985639_m1
TNFAIP6	Tumor necrosis factor, alpha-induced protein-6	Immunomodulation	Hs01113602_m1
VEGFA	Vascular endothelial growth factor	Angiogenesis	Hs00900055_m1

microwells, as previously reported (Kinney et al., 2012; Ungrin et al., 2008). Briefly, 6×10^5 cells were added to 24-well microwell inserts, let sit for 5 min and centrifuged at 1500 rpm for 10 min. After 18 h, spheroids were removed from the microwells and were either encapsulated in alginate or transferred to 6-well plates and cultured in suspension on a rotary orbital shaker, as previously described. At days 0, 4 and 7 of culture time, photographs were taken using a Leica DMI 3000 B microscope with a Nikon DXM 1200F digital camera. The area of the spheroids was measured using the area measurement algorithm from ImageJ software, after adjusting the threshold of the image pixels until the border of the spheroid.

2.3. Cellular encapsulation and cell retrieval from alginate beads

Alginic acid, sodium salt (Sigma) was dissolved in phosphate-buffered saline (PBS; Life Technologies) at 2.2% (w/v) with gentle shaking overnight and sterilized by filtration through 0.2 μm filters (Millipore). Both single MSC and preformed MSC spheroids were added to a syringe at a density of 4×10^6 and 6×10^6 cells, respectively, per mL of alginate. The alginate/cell solution was pumped at a 5 mL/h flow rate and extruded through a 250 μm nozzle into a 100 mM calcium chloride ($CaCl_2$) (Sigma) bath. Alginate droplets were detached from the tip of a N_2-driven bead generator (VAR J1 encapsulation unit; Nisco®) by applying a 0.8 bar pressure. The alginate beads generated were allowed to crosslink for approximately 10 min and were then collected from the $CaCl_2$ bath and washed twice with DMEM 1% A/A medium. Encapsulated cells were released from the alginate beads through incubation with a solution of 80 mM EDTA (Sigma) for 5 min at room temperature (RT).

2.4. Bovine serum albumin (BSA) release from alginate beads

To assess the rate of release of cytokines from an alginate matrix, a bovine serum albumin (BSA) solution (Sigma) was used as a model protein. To that purpose, alginate beads were prepared as described in Section 2.3., with 3 mg/mL BSA alginate solution instead of a cell/alginate solution. BSA released to the medium was quantified by the Bradford protocol. Briefly, the collected medium was incubated with Bradford reagent at the proportion 1:1 (v/v) for 10 min at RT. Absorbance was read at 595 nm on a spectrophotometer Infinite M200 PRO (Tecan) and BSA present in the supernatant was quantified using a calibration curve made with absorbance of solutions with known BSA concentrations.

2.5. Cell apoptosis and viability assessment

At day 4 of culture, single cells were collected after incubation with 0.25% trypsin EDTA at 37 °C for 10 min and cell viability was determined by flow cytometry using Annexin V-FITC/propidium iodide (PI) apoptosis detection kit (BD Pharmingen). Due to the inability to obtain an efficient dissociation of non-encapsulated MSC spheroids into single cells at day 7 of culture, we limited the data analysis provided in Fig. 3A and B to day 4 of cell culture. Dot plots display viable cells being negative for Annexin V and PI staining, early apoptotic cells being positive for Annexin V staining and negative for PI and dead cells being positive for PI staining. At days 4 and 7 of culture, the viability of MSC cultured as spheroids, encapsulated spheroids and encapsulated single cells was analyzed by double staining using a LIVE/DEAD viability/cytotoxicity kit (Life Technologies). Samples were incubated in PBS containing 2 μM calcein AM and 4 μM ethidium homodimer-1 for 1 h at RT, washed with PBS and immediately imaged under an optical microscope.

2.6. Resistance to oxidative stress

MSC cultured for 4 days as adherent monolayer, encapsulated single cells, spheroids and encapsulated spheroids were exposed to 3 mM H_2O_2 (Sigma) for 2 h to assess their resistance to oxidative stress. The number of viable cells was evaluated before and after exposure to H_2O_2 using either Trypan Blue exclusion method (for the monolayer and encapsulated single cells conditions) or CyQUANT Cell Proliferation Assay Kit (Invitrogen) (for the conditions comprising spheroids and encapsulated spheroids cell culture).

2.7. Real time (RT)-PCR for the expression of CXCL12, HGF, IL-6, TNFAIP6 and VEGFA

To evaluate the expression of angiogenic, chemotactic and anti-inflammatory genes, RT-PCR was performed with TaqMan Gene Analysis Assays (Life Technologies) for the primers GAPDH, CXCL12, HGF, IL-6, TNFAIP6 and VEGFA. Taqman primers of selected genes for RT-PCR are listed in Table 1.

Total RNA, harvested using RNeasy Mini Kit (Qiagen) at day 7 of cell culture, was reverse-transcribed to cDNA with the IScript cDNA synthesis kit (BioRad). cDNA was mixed with Taqman Gene Expression Mastermix (Applied Biosystems) and each Taqman gene-specific primer was subjected to the following PCR reaction performed in a RT-PCR equipment (StepOne, Applied Biosystems): 50 °C for 2 min, 95 °C for 10 min, 40 cycles of 95 °C for 15 s, 60 °C for 60 s.

The $2^{-D\Delta CT}$ method of relative quantification was used to determine the fold change in mRNA expression. GAPDH was used as the housekeeping gene and monolayer MSC as a baseline.

2.8. Quantification of secreted VEGF, HGF and IL-6 by ELISA

Secretion of VEGF, HGF and IL-6 was assessed in supernatant media collected upon cell culture between days 4 and 7. The supernatant samples were centrifuged at 1500 rpm for 10 min to remove cell debris, placed in new collection tubes and frozen at −80 °C. The amounts of total secreted proteins were determined by ELISA according to the manufacturer's instructions (Tebu-Bio).

2.9. Scratch wound healing assay

To assess the capability of L929 mouse fibroblasts (DSMZ, Braunschweig, Germany) to migrate into a wounded area in response to MSC-derived conditioned medium (CM), a scratch wound healing assay was performed. CM was prepared by incubating 6×10^5 MSC cultured as monolayer, encapsulated single cells, spheroids or encapsulated spheroids for 24 h in 1 mL of DMEM 1% A/A without FBS

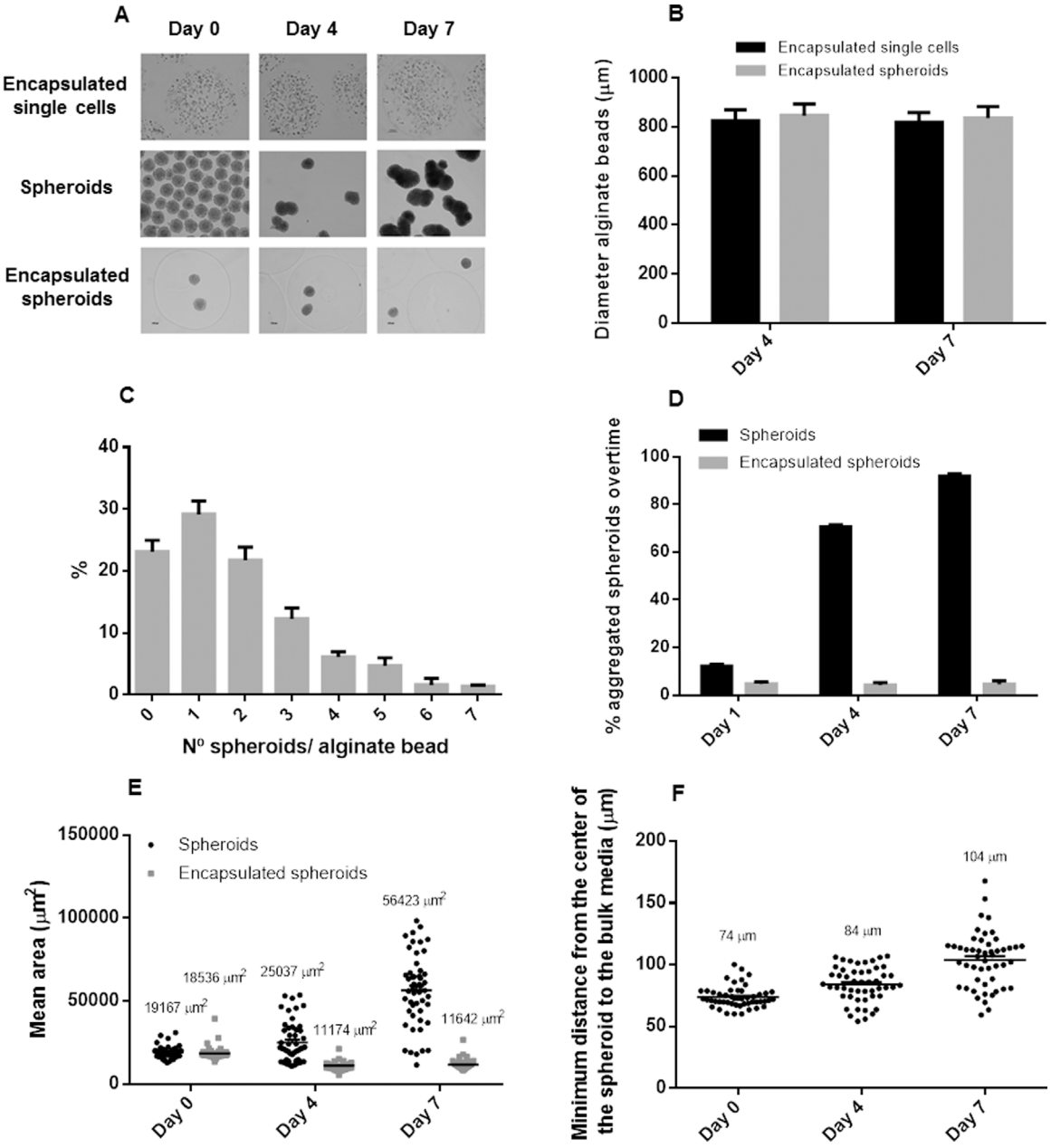

Fig. 2. Phase images of encapsulated single MSC, non-encapsulated and encapsulated spheroids in alginate beads at days 0, 4 and 7 of culture. Scale bar = 100 μm (A). The diameter of the alginate beads remains constant throughout culture time for both encapsulated single cells (826 ± 44.8 μm and 818 ± 40.1 μm at Days 4 and 7 of culture, respectively) and encapsulated spheroids (846 ± 47.0 μm and 836 ± 46.5 μm at Days 4 and 7, respectively) (n ≥ 30) (B). Distribution of number of spheroids per alginate bead. The majority of the beads contain one (29%) or two (22%) spheroids and the percentage of empty beads is of approximately 23% (n = 4) (C). Encapsulated spheroids evidence reduced agglomeration relatively to non-encapsulated spheroids (n = 4) (D). Values are represented as mean + SEM. The presence of an alginate matrix favors maintenance of spheroids with more uniform size overtime. While at day 0, non-encapsulated and encapsulated spheroids present a mean area of 19200 and 18500 μm^2, respectively, this value dramatically increases to 56400 μm^2 at day 7 when spheroids are cultured in the absence of an alginate matrix (E), with consecutive increase on the minimum distance from the center of non-encapsulated spheroids to the bulk medium overtime (F). 50 events were analyzed per time point.

supplementation, after which medium was collected, centrifuged at 1500 rpm for 10 min and stored at −80 °C until further use.

L929 mouse fibroblasts were cultured in 24-well plates at 1 × 10^4 cells/cm^2 and allowed to reach confluence. Cells were washed twice with PBS and serum-starved overnight. A linear defect was created by scratching the fibroblast monolayer with a 200 μL pipette tip, as described in (Liang et al., 2007). After immediately washing the wells to remove dislodged cells, CM was thawed and added to the wells.

Quantification of migration/proliferation was performed by measuring the distance moved by fibroblasts along the wounded area 4 h and 8 h after the scratch was performed. The percentage of wound closure was calculated applying the following equation:

$$\text{percentage of wound closure} = 1 - \frac{\text{diameter of the wound after x hours}}{\text{diameter of the wound immediately after the scratch was performed}}$$

2.10. Tube formation assay

The angiogenic potential of MSC-secreted factors was evaluated in a tube formation assay where the ability of human umbilical vein endothelial cells (HUVECs) (BD™) to form tubelike structures in the

presence of MSC-derived CM was measured by quantifying the length, number of tubes and branch points formed using ImageJ software. At day 4 of cell culture, MSC cultured as monolayer cells, encapsulated single MSC, non-encapsulated and encapsulated MSC spheroids were washed 3 times with DMEM 1% A/A and incubated in serum-free supplemented medium for 72 h. CM was collected, centrifuged at 1500 rpm for 10 min to remove cellular debris and stored at −80 °C until use in a Matrigel® assay (Arnaoutova and Kleinman, 2010). Briefly, 50 μL of Matrigel® Matrix Basement Membrane (Corning) was added to individual wells of a 96-well plate and allowed to polymerize for 1 h at 37 °C. 200 μL of MSC-derived CM containing 2×10^4 HUVECs was then added on top of the Matrigel® layer for 5 h before assaying tube formation.

To assess the ability of single or 3D-organized spheroids of MSC immobilized in an alginate matrix to secrete paracrine factors capable to diffuse through alginate and induce neighboring HUVECs to form networks of tubes, we performed a Matrigel® assay. A 2.2% (w/v) alginate solution containing single MSC or MSC spheroids was added to the bottom of 96-well plates, covered with 100 mM $CaCl_2$ and allowed to jellify for 20 min. The jellified alginate matrix with the encapsulated cells was washed and 200 μL of DMEM 10% FBS was added to the wells. After 4 days of culture, the Matrigel assay was performed. 50 μL Matrigel® were added on top of the alginate/cell matrix, allowed to polymerize for 1 h at 37 °C and 200 μL of DMEM 1% A/A containing 2×10^4 HUVECs were then added on the top of the Matrigel® layer. The highly growth factor-enriched EGM-2 medium (Lonza) was used as a positive control to culture HUVECs on Matrigel®.

2.11. Statistical analysis

Statistical analysis was performed using GraphPad Prism 6. Data are presented as mean + standard error of the mean (SEM). Two-way ANOVA was calculated between different experimental groups. Unless comparing unmatched groups, where one-way ANOVA was performed, repeated measures ANOVA was calculated. Tukey's multiple comparisons test was performed to determine statistically significant differences ($p < 0.05$).

3. Results

3.1. Controlling the size of MSC spheroids

Isolation of individual spheroids in alginate beads prevents their agglomeration overtime (Fig. 2A, D–F). Simultaneously, the seeding density of spheroids in alginate rendered less than 25% of empty beads (Fig. 2C). Whereas encapsulation in alginate beads with around 832 ± 6 μm of diameter (Fig. 2B) limits the percentage of aggregated spheroids to 5 ± 1% at day 7 of culture, non-encapsulated spheroids evidence 12 ± 1% aggregation as early as at day 1, reaching a level of 92 ± 1% aggregation at day 7 (Fig. 2D). Contrarily to the non-encapsulated spheroid condition, whose area increase from an initial value of approximately 19200 ± 500 μm^2 to 56400 ± 3100 μm^2 at day 7, simultaneously evidencing a larger spread on their size distribution, encapsulated spheroids present a more uniform size overtime, ranging from 18500 ± 500 μm^2 to 11600 ± 400 μm^2 at day 7 of culture (Fig. 2E). Moreover, progressive spheroid aggregation, observed for non-encapsulated spheroids, increases the minimal distance from the center of the spheroid to the bulk medium from a value of 74 ± 1 μm immediately post spheroid formation to 104 ± 4 μm at day 7 of culture (Fig. 2F).

While encapsulation was able to avoid aggregation of spheroids, the multipotency of MSC retrieved upon culture as encapsulated single cells or spheroids and non-encapsulated spheroids and monolayer cells for 7 days was qualitatively confirmed, a relevant issue as it has been suggested that the ability of cultured cells to retain their multilineage differentiation potential might be essential to potentiate their immunomodulatory activity (Ryan et al., 2014). The multipotency assessment of each of the four cell culture configurations under study was achieved upon specific induction with osteogenic, adipogenic and chondrogenic media for 14 days, followed by staining for alkaline phosphatase (ALP) and Von Kossa, Oil Red O or Alcian Blue and identification of calcium deposits (osteogenic lineage), lipid vacuoles (adipogenic lineage) and sulfated glycosaminoglycans (GAG) (chondrogenic lineage) (Supplementary Fig. 1), respectively. Despite evidence of multilineage differentiation potential, the 3D, compact cellular configuration associated with culture of MSC as spheroids hinders the ability to distinguish single cells to positively stain for differentiation markers of osteogenesis, adipogenesis and chondrogenesis in phase photos (Supplementary Fig. 1). This limitation has also been pointed out by Cerwinka and colleagues, for instance, who used immunohistochemistry studies to analyze 3D spheroids in cross-section (Cerwinka et al., 2012). Besides, the cell viability upon culture for 14 days in differentiation media was not assessed.

3.2. Cell viability and exposure to oxidative stress

The viability of MSC cultured as monolayer, non-encapsulated spheroids and encapsulated spheroids or encapsulated single cells was determined by flow cytometry upon Annexin V-FITC and PI labelling at day 4 of culture (Fig. 3A and B). Similar cell viability values were found for both monolayer and non-encapsulated spheroids. Still, when restricted to alginate beads, spheroids present a higher number of apoptotic cells and a lower number of viable cells relatively to non-encapsulated spheroids, evidencing a decrease of 89 ± 5% to 71 ± 10% of viable cells. Nevertheless, although both non-encapsulated and encapsulated spheroids evidence presence of dead cells within the spheroid structure at days 4 and 7 of cell culture, an extensive green-covered area, labelling viable cells, is observed in Fig. 3D.

To study if cellular encapsulation and/or culture as spheroids could improve MSC survival in conditions of oxidative stress, we exposed encapsulated single cells and spheroids, as well as non-encapsulated spheroids and monolayer adherent cells to 3 mM H_2O_2 for 2 h. The three 3D cell culture systems (encapsulated spheroids, encapsulated single cells and non-encapsulated spheroids) were less susceptible to oxidative stress than cells cultured as monolayer (survival of 72 ± 7, 69 ± 5 and 93 ± 12%, respectively, *vs* 23 ± 3%) (Fig. 3C). Not only culture of MSC as 3D structures seems to increase cell survival in an oxidative environment but also alginate shells might have contributed to create a protective effect over encapsulated cells.

3.3. Wound healing and angiogenic potential of 3D-cultured MSC

In response to cytokines, cells can migrate and proliferate onto a wounded area. Fibroblasts, for instance, are involved on synthesizing components of the ECM and can therefore be involved in tissue regeneration. In Fig. 4A, MSC-derived CM seems to provide chemotactic stimuli to fibroblasts, promoting wound closure overtime. Contrarily to DMEM 1% A/A (control), which lacks the paracrine factors secreted by MSC, CM collected upon culture of MSC in DMEM 1% A/A for 24 h in any of the four configurations assessed favored migration of fibroblasts into the wounded area (Figs. 4B and C). Particularly, encapsulated single cells-, non-encapsulated- and encapsulated spheroids-derived CM evidenced higher closure of the wounded area 8 h after the scratch was created relatively to monolayer-derived CM, as wound closure percentages of 40 ± 3, 39 ± 3 and 49 ± 6%, respectively, were evidenced relatively to a scratch closure of only 27 ± 1% in the presence of monolayer-derived CM. Moreover, as early as 4 h after the scratch was performed, encapsulated spheroid-derived CM led to significant wound closure relatively to DMEM 1% A/A, at a value of 26 ± 5%.

In our study, we used alginate as a delivery vehicle of bioactive factors being secreted by encapsulated MSC. We chose BSA as a model protein to study the release profile of encapsulated cytokines in alginate

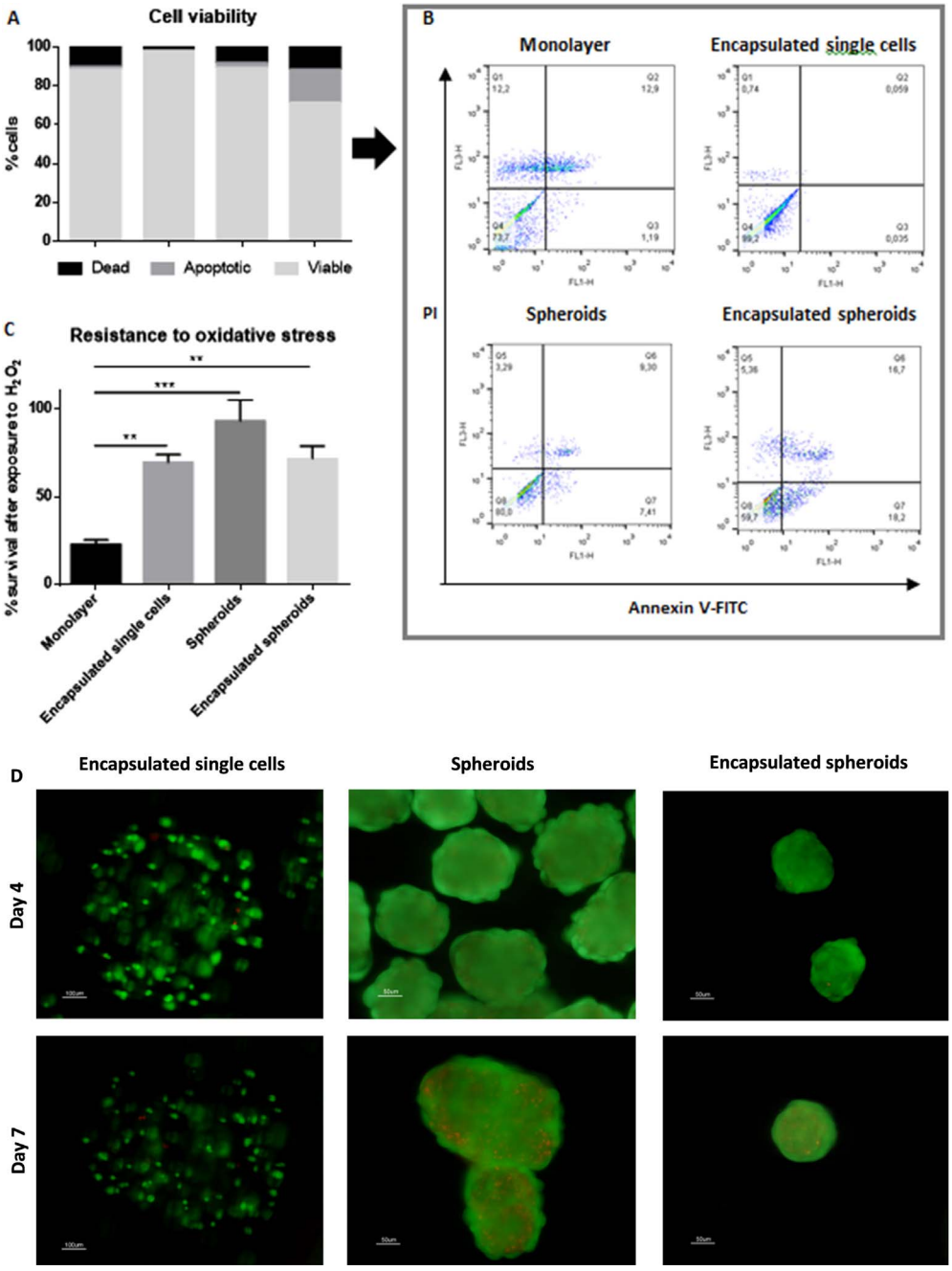

Fig. 3. Percentage of viable, apoptotic and dead cells cultured as monolayer, encapsulated single cells, spheroids and encapsulated spheroids (n = 4) (A) and respective dot plots of Annexin/PI staining (B). Percentage of cells that were able to sustain exposure to H_2O_2 (**p < 0.005, ***p < 0.0002, n = 4) (C). Values are represented as mean + SEM. Live/Dead images of encapsulated single cells, non-encapsulated spheroids and encapsulated spheroids at days 4 and 7 of culture. Green-labelled cells detected by calcein-AM indicate live cells whereas dead cells are stained in red by ethidium homodimer. Scale bar = 100 μm for encapsulated single cells and 50 μm for spheroids and encapsulated spheroids (D). (For interpretation of the references to colour in this figure legend, the reader is referred to the web version of this article.)

beads for 4 days, showing that a rapid release of 67 ± 5% occurs post 24 h of BSA encapsulation (Fig. 4D). In addition to providing a fast release of cellular secreted proteins, alginate does not seem to hinder the expression of the proangiogenic genes VEGF and HGF at day 7 of culture, as assessed by RT-PCR (Fig. 5A). Actually, we observe a higher expression of these genes for 3D configurations, *i.e.* spheroids, encapsulated single cells and encapsulated spheroids, and a significantly higher secretion of the correspondent angiogenic cytokines into the bulk media by encapsulated spheroids relatively to 2D monolayer cultured cells (Fig. 5B and C). However, no significant increase in expression of IL-6 and SDF-1α genes was observed between the MSC culture configurations assessed and, once assessed by ELISA measurements, the cytokine IL-6 actually evidences an increased secretion when MSC are cultured in a 2D monolayer configuration (Fig. 5D). Moreover, we observed the enhancing effect that MSC organization into spheroids, either non-encapsulated or encapsulated in alginate, has on upregulating the immunomodulatory factor TSG-6 (Fig. 5A), with fold change over monolayer culture of 39 ± 18 and 68 ± 35, respectively.

The angiogenic potential of MSC cultured as monolayer cells, encapsulated single cells, non-encapsulated and encapsulated spheroids was assessed in a tube formation assay (Fig. 6A), where the ability of HUVECs to form tubelike structures was assessed in the presence of MSC-derived CM. Greater tube length (Fig. 6B), number of tubes (Fig. 6C) and branch points (Fig. 6D) was observed when HUVECs were cultured in the presence of encapsulated spheroids-derived CM. Importantly, to better analyze the angiogenic properties of BM MSC, a tube formation assay was performed in direct co-culture with HUVECs (Fig. 6E). Only encapsulated MSC (single MSC and 3D spheroids) were tested to ensure that the effects observed were a direct consequence of the secretome and not due to cell-to-cell contact. Culture of HUVECs in EGM-2 medium on top of Matrigel® was used as example of a high case scenario boundary considering the potential of formation of tubes by

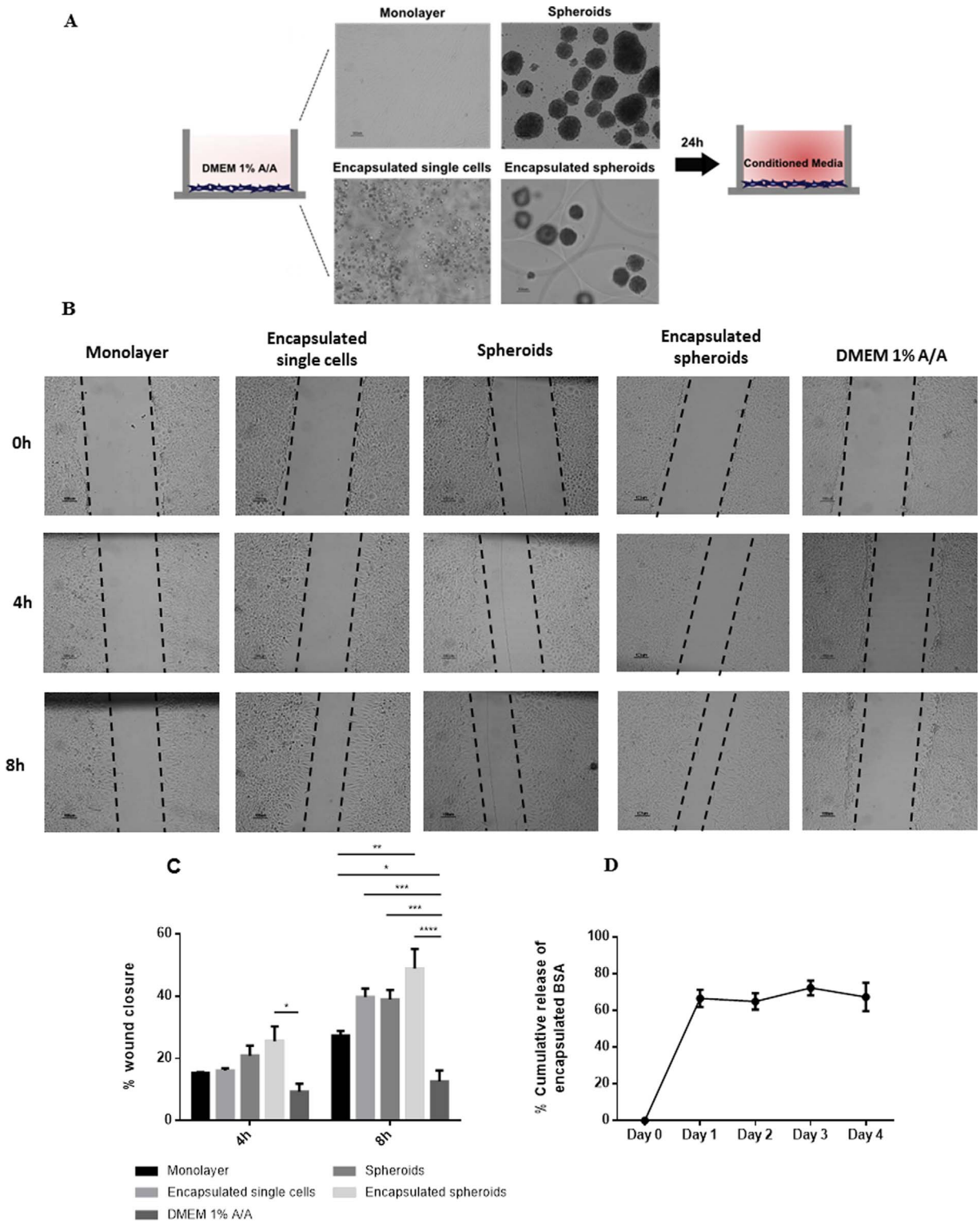

Fig. 4. Representative images of migration of L929 fibroblasts into a wounded area created by mechanical disruption with a 200 μL tip, immediately (0 h), 4 h or 8 h after scratching, in the presence of MSC-derived CM (B). CM was collected after culturing MSC as monolayer, encapsulated single cells, spheroids and encapsulated spheroids for 24 h in medium without serum (DMEM 1% A/A) (A) and added to a wounded monolayer of fibroblasts. As control, non-conditioned DMEM without FBS (DMEM 1% A/A) was used. Migration of fibroblasts was increased in the presence of encapsulated spheroids-derived CM (*$p < 0.05$, **$p < 0.005$, ***$p < 0.0005$, ****$p < 0.0001$, $n = 3$) (C). Release profile of encapsulated BSA from alginate beads ($n \geq 3$) (D). Values are represented as mean + SEM.

HUVECs. Co-culture of encapsulated single cells or spheroids with HUVECs seeded on top of Matrigel® in DMEM 1% A/A allowed to assess the angiogenic potential of MSC in the absence of the growth factor-enriched EGM-2 medium. Encapsulated spheroids promoted formation of a more interconnected network of tubes as both the number of tubes and nodes increased in the presence of spheroids relatively to single encapsulated MSC (Fig. 6F–H).

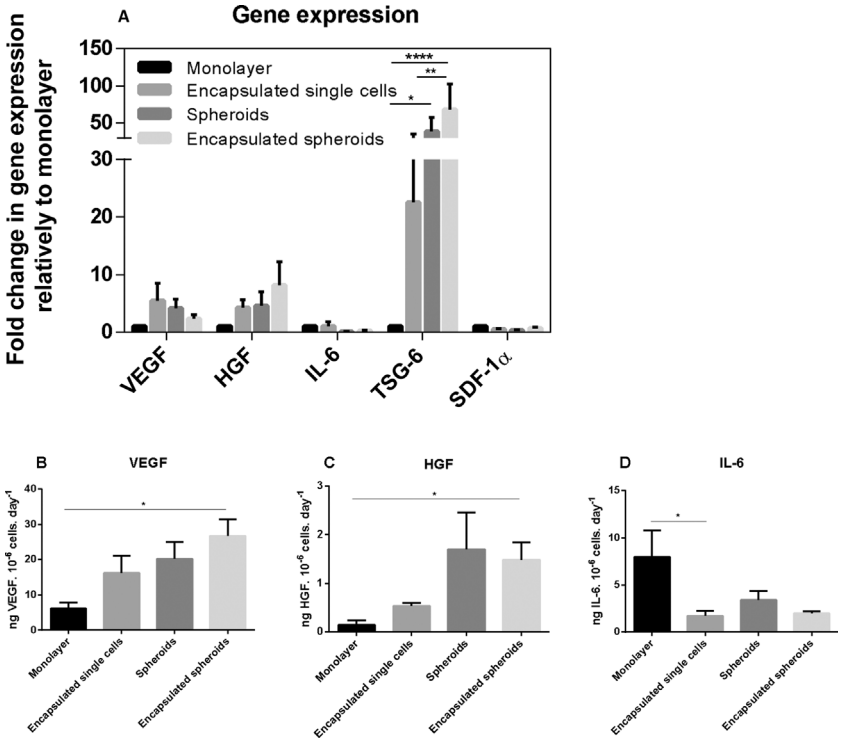

Fig. 5. Quantification of genes (VEGF, HGF, IL-6, TSG-6, SDF-1α) involved in the paracrine activity of BM MSC cultured as monolayer, encapsulated single cells, spheroids and encapsulated spheroids (*p < 0.05, **p < 0.005,****p < 0.0001, n = 4) (A). Secretion of angiogenic factors − VEGF (B), HGF (C), and IL-6 (D) − was determined in MSC-CM. Values are represented as mean + SEM (*p < 0.05, n = 4).

4. Discussion

When considering the development of therapeutic cell products, namely MSC-derived, the predictability of the behavior of culture systems needs to be increased. Importantly, this higher control over experimental conditions should be able to maximize the paracrine activity of cultured cells, one of the key features underlying the therapeutic potential of MSC. In our study, we explored the paracrine potential of BM-derived MSC organized as spheroids or as alginate-encapsulated MSC and provide a side-by-side comparison of their wound healing potential with cells cultured as monolayer, the conventional 2D configuration used for cell culture.

4.1. Encapsulation as a tool to limit aggregation of MSC spheroids

The current study exploits a controllable system for delivery of MSC spheroids, capable of producing trophic factors involved in a wound healing response, through encapsulation in alginate beads. Encapsulated spheroids range from an area of 18500 ± 500 μm^2 at day 0–11,600 ± 400 μm^2 at day 7 of cell culture (Fig. 2E), corresponding roughly to spherical spheroids with a diameter of 153 ± 2 and 121 ± 2 μm, respectively. The observed reduction of the encapsulated spheroids size has been suggested to be a result of compaction of multicellular aggregates (Tsai et al., 2015). On the other hand, non-encapsulated MSC spheroids show progressive aggregation of individual spheroids overtime, thus resulting in formation of spheroids with irregular shape and higher size (Fig. 2A, D–F). Such spheroid heterogeneity might lead to uncontrolled cell properties and unpredictable secretome profile. Indeed, it has been shown that for the use of spheroids in drug testing models, culture of morphologically homogeneous spheroids must be attained in order to be biologically relevant (Freyer and Sutherland, 1986; Zanoni et al., 2016). This fact positions the use of hydrogel-based strategies to encapsulate spheroids as a valuable strategy to achieve higher control over the spheroids size.

Concerning the contributions of MSC-secreted trophic factors for wound repair and regeneration, it has been hypothesized that creation of a hypoxic environment in the spheroids core is responsible for enhanced angiogenesis (Bhang et al., 2011) and activation of cellular mechanisms that constitute a survival advantage under oxidative stress conditions (Zhang et al., 2012; Zhao et al., 2015a,b). Although not statistically significant, RT-PCR data of spheroids, encapsulated spheroids or single cells show increased expression of genes involved in angiogenesis, namely VEGF and HGF, in comparison to monolayer cells. Beyond hypoxia-driven signaling, the enhanced angiogenic potential of spheroids and encapsulated cells might be due to other mechanisms. Indeed, in our study, MSC cultured as 500-cell spheroids present a diameter far below the 300 μm diameter reported in the literature to be responsible for the development of oxygen gradients within cell aggregates (Sen et al., 2001). Even at the more stringent conditions, at day 7 of non-encapsulated spheroids culture, when high levels of aggregation are observed, the mean minimum distance from the center of the spheroid to the bulk medium is of approximately 104 ± 3 μm (Fig. 2F). In addition to hypoxia-induced stress, intercellular adhesions such as the ones mediated by E-cadherin (Lee et al., 2012) have been pointed out to be responsible for enhancing the angiogenic potential of MSC.

It has been reported that necrotic areas could be formed within the core of spheroids with large diameters due to nutrients and oxygen limited diffusion (Sen et al., 2001). To minimize this effect, we preformed MSC spheroids whose initial diameter of approximately 150 μm is within the limits of oxygen diffusion (Sen et al., 2001; Wu et al., 2014). We hypothesize that a compromise on the spheroid diameter should be attained in order to maximize cellular viability while their paracrine activity is potentiated.

Noteworthy, alginate encapsulation can also pose diffusion limitations, despite the oxygen permeability in a 2% alginate solution (3.43×10^{-14} mol/cm/mmHg/s) has been reported to be approximately three times higher than that in tissues (1.24×10^{-14} mol/cm/mmHg/s) (Johnson et al., 2009). Still, such restraint to diffusion can lead to oxygen limitations responsible for hypoxia-induced stress, which can contribute to understand the results promoting the wound healing response in encapsulated single cells.

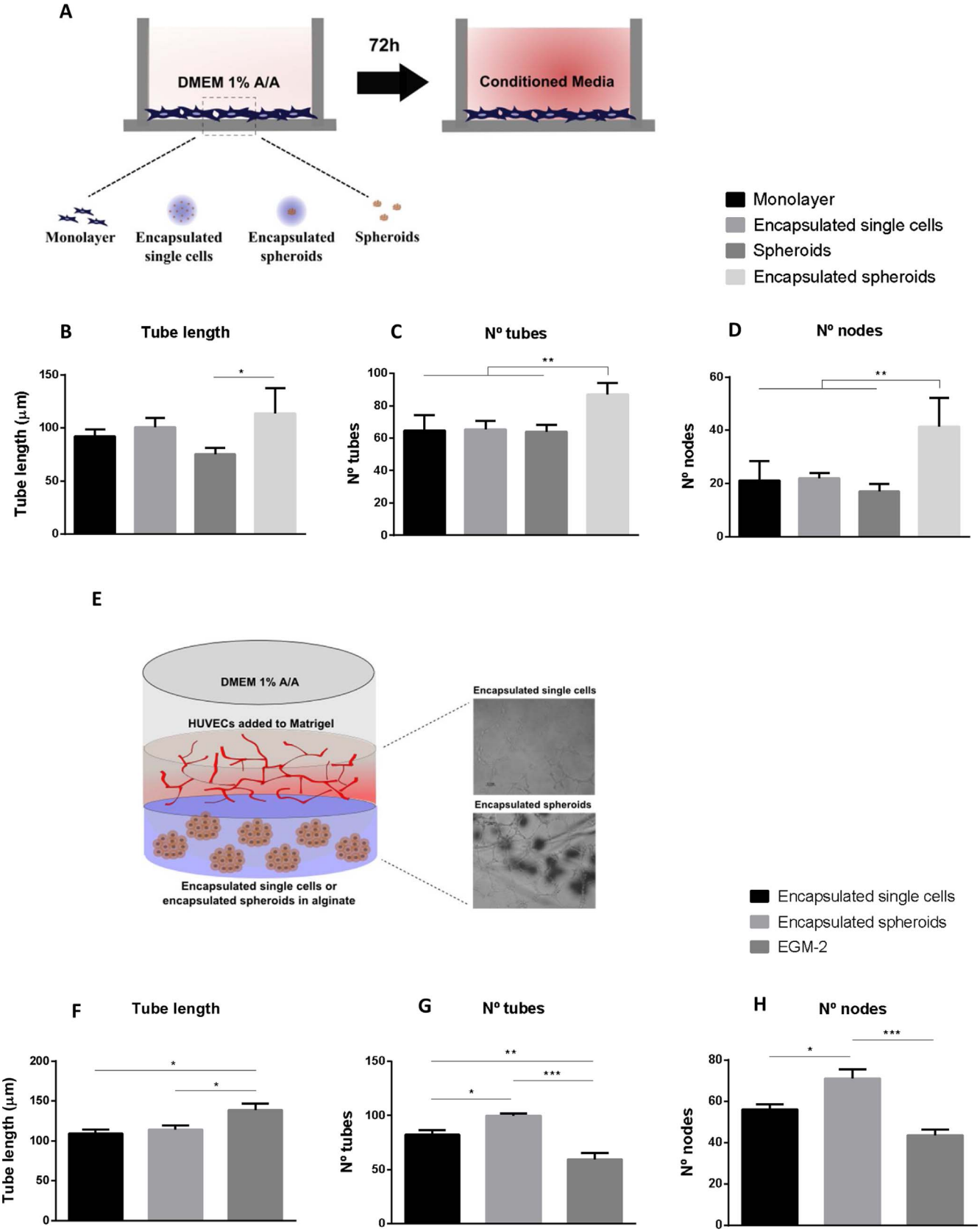

Fig. 6. Tubelike structures formed by HUVECs in the presence of CM collected upon culture of MSC as monolayer cells, encapsulated single MSC, non-encapsulated and encapsulated spheroids for 72 h in DMEM 1% A/A (A). The tube length (B), number of tubes (C) and number of nodes (D) were analyzed post 5 h (*$p < 0.05$, **$p < 0.01$, $n = 4$; single biological donor, with replicates). Values are represented as mean + SD. Tubelike structures formed by HUVECs in co-culture with single MSC and spheroids encapsulated in an alginate disk. HUVECs were added to Matrigel® seeded on top of an alginate layer containing encapsulated MSC (E) and their tube length (F), number of tubes (G) and number of nodes (H) were analyzed post 5 h. To assess the angiogenic potential of single MSC *vs* 3D spheroids encapsulated in alginate, MSC were initially encapsulated in an alginate hydrogel and cultured for 4 days. HUVECs were then added to an upper Matrigel® layer in DMEM 1% A/A. HUVECs cultured alone on Matrigel® in the presence of EGM-2 media were used as control (*$p < 0.05$, **$p < 0.01$, ***$p < 0.0005$, $n \geq 4$). Values are represented as mean + SEM.

4.2. 3D cell culture as a means to improve resistance against oxidative stress injury

In the harsh environment of injured tissues, oxidative stress is thought to lead to cell death. After wounding, ROS, including H_2O_2, are produced, leading to excessive oxidative damage that contributes to the pathogenesis of chronic wounds (Schafer and Werner, 2008). We observed that culture of MSC as spheroids, even if not protected by an alginate shell, increases their resistance to oxidative stress (Fig. 3C). Zhang and colleagues (Zhang et al., 2012) have shown that upregulated expression of hypoxia-adaptive genes, such as HIFs, superoxide dismutase-2 and VEGF in spheroids, might be responsible for higher resistance to oxidative stress relatively to monolayer cells. The increased expression of stanniocalcin-1 by spheroids (Bartosh et al., 2010) has been reported to be capable of suppressing ROS (Wang et al., 2009). On the other hand, the higher percentage of cell survival to oxidative stress when single cells are encapsulated might be attributed to a protective effect of the alginate structure on the entrapped cells. Furthermore, although oxidative damage in injured tissues can lead to cell death, lack of oxygenation due to vasculature disruption is also a major issue that needs to be addressed in order to favor tissue remodeling (Nauta et al., 2014). Preservation of ECM and the enhanced proangiogenic potential of 3D spheroid structures might improve survival under ischemic conditions.

4.3. Alginate encapsulation – a delivery vehicle of encapsulated MSC-secreted trophic factors

In this study, we selected non-functionalized alginate as a cell encapsulation vehicle to study the effect of having BM MSC cultured as spheroids *versus* single cells on their paracrine potential, circumventing the introduction of additional cues that a non-inert material would provide. Other studies, however, have shown that MSC spheroids encapsulated in arginine-glycine-aspartic acid (RGD)-modified alginate exhibit enhanced survival and VEGF secretion. Nevertheless, the 3D spheroid configuration is lost over culture time in these functionalized alginate matrices (Ho et al., 2016), which might limit the anti-inflammatory behavior of MSC, whose expression of immunomodulatory factors is thought to be favored when MSC are compacted in a 3D spheroid configuration (Bartosh et al., 2010). Furthermore, the alginate burst release behavior of the model protein BSA positions alginate as an interesting inert material to allow diffusion of proteins into the surrounding environment while the secretory machinery of MSC is working. Alternatively to preselect a group of proteins to be delivered in an *in vivo* setting, through cellular encapsulation, we can rather take advantage of the plethora of bioactive compounds that constitute the MSC secretome. It has been shown that sequential delivery of three growth factors (VEGF, platelet-derived growth factor-BB (PDGF-BB) and TGF-β1) from alginate scaffolds resulted in better vascularization *in vivo* than instantaneously or single factor delivery (Freeman and Cohen, 2009).

Moreover, through encapsulation, retention of MSC at an implanted site can be increased (Ceccaldi et al., 2012; Landázuri et al., 2012), enhancing cellular communication with the surrounding wounded environment. Interactions between different cell types are essential to achieve fully functional tissues, which led us to study the paracrine interactions of MSC cultured as single cells or as 3D spheroids with HUVECs and fibroblasts.

Whereas encapsulated single MSC-derived CM seems to at least equal the enhancing effects that non-encapsulated MSC-secreted factors have on promoting fibroblast migration, similarly to what Bussche and co-workers (Bussche et al., 2015) have observed with encapsulated single equine MSC, we showed that encapsulation of MSC spheroids can boost this effect.

In addition to cellular migration into the wounded site, which is critical during the wound healing process, angiogenesis is essential to achieve an efficient healing as it allows delivery of nutrients and oxygen to living tissues. We observed that CM harvested from encapsulated MSC spheroids for 72 h in DMEM 1% A/A enhances the ability of HUVECs to form tubes, as observed by a statistically significant greater number of tubes and branch points relatively to monolayer, encapsulated single MSC and non-encapsulated spheroids (Fig. 6A–D). Interestingly, direct co-culture of HUVECs with encapsulated single MSC or spheroids increases the formation of tubelike structures, therefore highlighting the angiogenic potential of encapsulated MSC (Fig. 6E–H). Similar reports have demonstrated that MSC entrapped in RGD-functionalized alginate increases the ability of neighboring HUVECs to form tubelike structures and enhances endothelial cell invasion *in vitro* (Bidarra et al., 2010). However, although having MSC encapsulated as single cells in alginate beads has been shown to promote an increase of 70% in vascular density relatively to a more modest value of 22% when cells were delivered as non-encapsulated cells in the setting of mice hindlimb ischemia (Landázuri et al., 2012), combining culture of MSC as 3D spheroids with encapsulation within an alginate matrix could potentially further exploit the paracrine potential of MSC. Indeed, in our study, we showed that HUVECs in co-culture with MSC spheroids encapsulated in alginate can contribute to formation of an interconnected network of tubes, with higher number of tubes and branch points being formed in comparison to co-culture with encapsulated single cells (Fig. 6F–H). The lack of cell–cell contact between MSC and HUVECs in these experiments suggests that paracrine factors secreted by MSC, particularly when cultured as encapsulated spheroids, such as VEGF and HGF, whose gene expression (Fig. 5A) and protein secretion (Fig. 5B-C) was detected at day 7 of cell culture, might potentiate the function of endothelial cells.

Gene expression of immunomodulatory factors was also assessed, particularly IL-6 and TSG-6 (Fig. 5A), as they play a role in wound healing, namely on mediating anti-inflammatory responses (Djouad et al., 2007; Lee et al., 2014). Culture of MSC as spheroids has proven to be an effective way to increase the expression of such immunomodulatory factors (Bartosh et al., 2010; YlÖstalo et al., 2012; Zimmermann and Mcdevitt, 2014), although, in our study, we detected higher secreted levels of IL-6 when MSC are cultured in a 2D monolayer configuration (Fig. 5D). Importantly, enhanced expression of TSG-6 by MSC spheroids relatively to monolayer cultures contributes to suppress inflammatory reactions (Bartosh et al., 2010), which are exacerbated in a wounding setting where the host immune system is activated to respond to injury. Indeed, the efficacy of MSC on reducing inflammation has been shown to be proportional to the mRNA levels of the anti-inflammatory protein TSG-6 (Lee et al., 2014, p. 6; Sala et al., 2015). Knock-down experiments showed that improvement of the cardiac function after myocardial infarction is, at least in part, mediated by MSC secretion of TSG-6 (Lee et al., 2009). In our study, we showed that both encapsulated and non-encapsulated spheroids express high levels of the TSG-6 gene (Fig. 5A), although the former evidenced higher expression, which might be at least in part explained by the higher number of apoptotic cells detected in Fig. 3A and B, as cellular apoptosis has been linked to activation of anti-inflammatory signals (Bartosh et al., 2010; YlÖstalo et al., 2012). This suggests that MSC culture either as 3D spheroids or as biomaterial-encapsulated cells could potentially increase the immunomodulatory potential of these cells, as recently reviewed in (Follin et al., 2016).

Overall, in the setting of tissue repair and regeneration processes, whose time course takes days to weeks, retention of cells with enhanced proangiogenic, anti-inflammatory and chemotactic capabilities at an injured site, protected from a harsh oxidative stress environment characteristic of wounded sites, while maintaining controllable size properties through encapsulation within an alginate matrix, might extend the therapeutic potential of MSC.

Conflict of interest

The authors declare no commercial or financial conflict of interest.

Acknowledgements

The authors acknowledge funding from (i) Portuguese Foundation for Science and Technology (FCT), Portugal State Budget and (ii) Lisbon's Regional Operational Programme 2014-2020 (PORL2020), European structural and investment funds − European commission. Namely, the authors thank PORL2020 and FCT funding of iBB-Institute for Bioengineering and Biosciences (FCT reference: UID/BIO/04565/2013 and POL2020 reference 007317, including iBB grant iBB/2015/18), and the Research and Development Project Grant from the Joint Activities Programme "PRECISE", reference 016394. The authors also thank FCT for granting scholarships SFRH/BD/52000/2012, SFRH/BSAB/128442/2017 and MIT Portugal Program, as well to the European Commission by funding of Discoveries Centre for Regenerative and Precision Medicine, Program Teaming Health H2020-WIDESPREAD-2014, reference 664558. The authors declare no commercial or financial conflict of interest.

Appendix A. Supplementary data

Supplementary data associated with this article can be found, in the online version, at http://dx.doi.org/10.1016/j.jbiotec.2017.09.020.

References

Arnaoutova, I., Kleinman, H.K., 2010. In vitro angiogenesis: endothelial cell tube formation on gelled basement membrane extract. Nat. Protoc. 5, 628–635. http://dx.doi.org/10.1038/nprot.2010.6.

Bartosh, T.J., Ylostalo, J.H., Mohammadipoor, A., Bazhanov, N., Coble, K., Claypool, K., Lee, R.H., Choi, H., Prockop, D.J., 2010. Aggregation of human mesenchymal stromal cells (MSCs) into 3D spheroids enhances their antiinflammatory properties. Proc. Natl. Acad. Sci. 107, 13724–13729. http://dx.doi.org/10.1073/pnas.1008117107.

Bartosh, T.J., Ylöstalo, J.H., Bazhanov, N., Kuhlman, J., Prockop, D.J., 2013. Dynamic compaction of human mesenchymal stem/precursor cells into spheres self-activates caspase-dependent IL1 signaling to enhance secretion of modulators of inflammation and immunity (PGE2, TSG6, and STC1): activation of IL1-signaling in MSC Spheres. Stem Cells 31, 2443–2456. http://dx.doi.org/10.1002/stem.1499.

Bhang, S.H., Cho, S.-W., La, W.-G., Lee, T.-J., Yang, H.S., Sun, A.-Y., Baek, S.-H., Rhie, J.-W., Kim, B.-S., 2011. Angiogenesis in ischemic tissue produced by spheroid grafting of human adipose-derived stromal cells. Biomaterials 32, 2734–2747. http://dx.doi.org/10.1016/j.biomaterials.2010.12.035.

Bhang, S.H., Lee, S., Shin, J.-Y., Lee, T.-J., Kim, B.-S., 2012. Transplantation of cord blood mesenchymal stem cells as spheroids enhances vascularization. Tissue Eng. Part A 18, 2138–2147. http://dx.doi.org/10.1089/ten.tea.2011.0640.

Bidarra, S.J., Barrias, C.C., Barbosa, M.A., Soares, R., Granja, P.L., 2010. Immobilization of human mesenchymal stem cells within RGD-Grafted alginate microspheres and assessment of their angiogenic potential. Biomacromolecules 11, 1956–1964. http://dx.doi.org/10.1021/bm100264a.

Blacher, S., Erpicum, C., Lenoir, B., Paupert, J., Moraes, G., Ormenese, S., Bullinger, E., Noel, A., 2014. Cell invasion in the spheroid sprouting assay: a spatial organisation analysis adaptable to cell behaviour. PLoS One 9, e97019. http://dx.doi.org/10.1371/journal.pone.0097019.

Broughton, G., Janis, J.E., Attinger, C.E., 2006. Wound healing: an overview. Plast. Reconstr. Surg. 117, 1e. http://dx.doi.org/10.1097/01.prs.0000222562.60260.f9.

Bussche, L., Harman, R.M., Syracuse, B.A., Plante, E.L., Lu, Y.-C., Curtis, T.M., Ma, M., Van de Walle, G.R., 2015. Microencapsulated equine mesenchymal stromal cells promote cutaneous wound healing in vitro. Stem Cell Res. Ther. 6. http://dx.doi.org/10.1186/s13287-015-0037-x.

Caplan, A.I., Dennis, J.E., 2006. Mesenchymal stem cells as trophic mediators. J. Cell. Biochem. 98, 1076–1084. http://dx.doi.org/10.1002/jcb.20886.

Ceccaldi, C., Fullana, S.G., Alfarano, C., Lairez, O., Calise, D., Cussac, D., Parini, A., Sallerin, B., 2012. Alginate scaffolds for mesenchymal stem cell cardiac therapy: influence of alginate composition. Cell Transplant. 21, 1969–1984. http://dx.doi.org/10.3727/096368912x647252.

Cerwinka, W.H., Sharp, S.M., Boyan, B.D., Zhau, H.E., Chung, L.W., Yates, C., 2012. Differentiation of human mesenchymal stem cell spheroids under microgravity conditions. Cell Regen. 1, 2.

Di Nicola, M., Carlo-Stella, C., Magni, M., Milanesi, M., Longoni, P.D., Matteucci, P., Grisanti, S., Gianni, A.M., 2002. Human bone marrow stromal cells suppress T-lymphocyte proliferation induced by cellular or nonspecific mitogenic stimuli. Blood 99, 3838–3843.

Ding, S., Merkulova-Rainon, T., Han, Z.C., Tobelem, G., 2003. HGF receptor up-regulation contributes to the angiogenic phenotype of human endothelial cells and promotes angiogenesis in vitro. Blood 101, 4816–4822.

Djouad, F., Charbonnier, L.-M., Bouffi, C., Louis-Plence, P., Bony, C., Apparailly, F., Cantos, C., Jorgensen, C., Noël, D., 2007. Mesenchymal stem cells inhibit the differentiation of dendritic cells through an interleukin-6-dependent mechanism. Stem Cells 25, 2025–2032. http://dx.doi.org/10.1634/stemcells.2006-0548.

Eftekharzadeh, B., Khodagholi, F., Abdi, A., Maghsoudi, N., 2010. Alginate protects NT2 neurons against H2O2-induced neurotoxicity. Carbohydr. Polym. 79, 1063–1072. http://dx.doi.org/10.1016/j.carbpol.2009.10.040.

Ferrara, N., 2001. Role of vascular endothelial growth factor in regulation of physiological angiogenesis. Am. J. Physiol.-Cell Physiol. 280, C1358–C1366.

Follin, B., Juhl, M., Cohen, S., Perdersen, A.E., Kastrup, J., Ekblond, A., 2016. Increased paracrine immunomodulatory potential of mesenchymal stromal cells in three-dimensional culture. Tissue Eng. Part B Rev. 22, 322–329. http://dx.doi.org/10.1089/ten.teb.2015.0532.

Freeman, I., Cohen, S., 2009. The influence of the sequential delivery of angiogenic factors from affinity-binding alginate scaffolds on vascularization. Biomaterials 30, 2122–2131. http://dx.doi.org/10.1016/j.biomaterials.2008.12.057.

Freyer, J.P., Sutherland, R.M., 1986. Proliferative and clonogenic heterogeneity of cells from EMT6/Ro multicellular spheroids induced by the glucose and oxygen supply. Cancer Res. 46, 3513–3520.

Gerritsen, M.E., 2005. HGF and VEGF: a dynamic duo. Circ. Res. 96, 272–273. http://dx.doi.org/10.1161/01.RES.0000157575.66295.e0.

Gnecchi, M., 2006. Evidence supporting paracrine hypothesis for Akt-modified mesenchymal stem cell-mediated cardiac protection and functional improvement. FASEB J. 20, 661–669. http://dx.doi.org/10.1096/fj.05-5211com.

Hashimoto, T., Suzuki, Y., Tanihara, M., Kakimaru, Y., Suzuki, K., 2004. Development of alginate wound dressings linked with hybrid peptides derived from laminin and elastin. Biomaterials 25, 1407–1414. http://dx.doi.org/10.1016/j.biomaterials.2003.07.004.

Ho, S.S., Murphy, K.C., Binder, B.Y.K., Vissers, C.B., Leach, J.K., 2016. Increased survival and function of mesenchymal stem cell spheroids entrapped in instructive alginate hydrogels. Stem Cells Transl. Med. 5, 773–781. http://dx.doi.org/10.5966/sctm.2015-0211.

Janssens, K., Slaets, H., Hellings, N., 2015. Immunomodulatory properties of the IL-6 cytokine family in multiple sclerosis: immunomodulatory role of the IL-6 family in MS. Ann. N. Y. Acad. Sci. 1351, 52–60. http://dx.doi.org/10.1111/nyas.12821.

Johnson, A.S., Fisher, R.J., Weir, G.C., Colton, C.K., 2009. Oxygen consumption and diffusion in assemblages of respiring spheres: performance enhancement of a bioartificial pancreas. Chem. Eng. Sci. 64, 4470–4487. http://dx.doi.org/10.1016/j.ces.2009.06.028.

Khanna, S., Biswas, S., Shang, Y., Collard, E., Azad, A., Kauh, C., Bhasker, V., Gordillo, G.M., Sen, C.K., Roy, S., 2010. Macrophage dysfunction impairs resolution of inflammation in the wounds of diabetic mice. PLoS One 5, e9539. http://dx.doi.org/10.1371/journal.pone.0009539.

Kinney, M.A., Saeed, R., McDevitt, T.C., 2012. Systematic analysis of embryonic stem cell differentiation in hydrodynamic environments with controlled embryoid body size. Integr. Biol. 4, 641. http://dx.doi.org/10.1039/c2ib00165a.

Kwon, H.M., Hur, S.-M., Park, K.-Y., Kim, C.-K., Kim, Y.-M., Kim, H.-S., Shin, H.-C., Won, M.-H., Ha, K.-S., Kwon, Y.-G., Lee, D.H., Kim, Y.-M., 2014. Multiple paracrine factors secreted by mesenchymal stem cells contribute to angiogenesis. Vascul. Pharmacol. 63, 19–28. http://dx.doi.org/10.1016/j.vph.2014.06.004.

Kwon, S.H., Bhang, S.H., Jang, H.-K., Rhim, T., Kim, B.-S., 2015. Conditioned medium of adipose-derived stromal cell culture in three-dimensional bioreactors for enhanced wound healing. J. Surg. Res. 194, 8–17. http://dx.doi.org/10.1016/j.jss.2014.10.053.

Landázuri, N., Levit, R.D., Joseph, G., Ortega-Legaspi, J.M., Flores, C.A., Weiss, D., Sambanis, A., Weber, C.J., Safley, S.A., Taylor, W.R., 2012. Alginate microencapsulation of human mesenchymal stem cells as a strategy to enhance paracrine-mediated vascular recovery after hindlimb ischaemia: encapsulated human MSCs enhance revascularization. J. Tissue Eng. Regen. Med. 222–232. http://dx.doi.org/10.1002/term.1680.

Lee, R.H., Pulin, A.A., Seo, M.J., Kota, D.J., Ylostalo, J., Larson, B.L., Semprun-Prieto, L., Delafontaine, P., Prockop, D.J., 2009. Intravenous hMSCs improve myocardial infarction in mice because cells embolized in lung are activated to secrete the anti-inflammatory protein TSG-6. Cell Stem Cell 5, 54–63. http://dx.doi.org/10.1016/j.stem.2009.05.003.

Lee, K., Silva, E.A., Mooney, D.J., 2010. Growth factor delivery-based tissue engineering: general approaches and a review of recent developments. J. R. Soc. Interface 8, 153–170. http://dx.doi.org/10.1098/rsif.2010.0223.

Lee, E.J., Park, S.J., Kang, S.K., Kim, G.-H., Kang, H.-J., Lee, S.-W., Jeon, H.B., Kim, H.-S., 2012. Spherical bullet formation via E-cadherin promotes therapeutic potency of mesenchymal stem cells derived from human umbilical cord blood for myocardial infarction. Mol. Ther. 20, 1424–1433. http://dx.doi.org/10.1038/mt.2012.58.

Lee, R.H., Yu, J.M., Foskett, A.M., Peltier, G., Reneau, J.C., Bazhanov, N., Oh, J.Y., Prockop, D.J., 2014. TSG-6 as a biomarker to predict efficacy of human mesenchymal stem/progenitor cells (hMSCs) in modulating sterile inflammation in vivo. Proc. Natl. Acad. Sci. 111, 16766–16771. http://dx.doi.org/10.1073/pnas.1416121111.

Liang, C.-C., Park, A.Y., Guan, J.-L., 2007. In vitro scratch assay: a convenient and inexpensive method for analysis of cell migration in vitro. Nat. Protoc. 2, 329–333. http://dx.doi.org/10.1038/nprot.2007.30.

Liu, H., Liu, S., Li, Y., Wang, X., Xue, W., Ge, G., Luo, X., 2012. The role of SDF-1-CXCR4/CXCR7 axis in the therapeutic effects of hypoxia-preconditioned mesenchymal stem cells for renal ischemia/reperfusion injury. PLoS One 7, e34608. http://dx.doi.org/10.1371/journal.pone.0034608.

Matyash, M., Despang, F., Mandal, R., Fiore, D., Gelinsky, M., Ikonomidou, C., 2012. Novel soft alginate hydrogel strongly supports neurite growth and protects neurons

against oxidative stress. Tissue Eng. Part A 18, 55–66. http://dx.doi.org/10.1089/ten.tea.2011.0097.

Nauta, T., van Hinsbergh, V., Koolwijk, P., 2014. Hypoxic signaling during tissue repair and regenerative medicine. Int. J. Mol. Sci. 15, 19791–19815. http://dx.doi.org/10.3390/ijms151119791.

Potier, E., Ferreira, E., Meunier, A., Sedel, L., Logeart-Avramoglou, D., Petite, H., 2007. Prolonged hypoxia concomitant with serum deprivation induces massive human mesenchymal stem cell death. Tissue Eng. 13, 1325–1331. http://dx.doi.org/10.1089/ten.2006.0325.

Ryan, A.E., Lohan, P., O'Flynn, L., Treacy, O., Chen, X., Coleman, C., Shaw, G., Murphy, M., Barry, F., Griffin, M.D., Ritter, T., 2014. Chondrogenic differentiation increases antidonor immune response to allogeneic mesenchymal stem cell transplantation. Mol. Ther. 22, 655–667. http://dx.doi.org/10.1038/mt.2013.261.

Safley, S.A., Cui, H., Cauffiel, S., Tucker-Burden, C., Weber, C.J., 2008. Biocompatibility and immune acceptance of adult porcine islets transplanted intraperitoneally in diabetic NOD mice in calcium alginate poly-L-lysine microcapsules versus barium alginate microcapsules without poly-L-lysine. J. Diabetes Sci. Technol. 2, 760–767.

Sala, E., Genua, M., Petti, L., Anselmo, A., Arena, V., Cibella, J., Zanotti, L., D'Alessio, S., Scaldaferri, F., Luca, G., Arato, I., Calafiore, R., Sgambato, A., Rutella, S., Locati, M., Danese, S., Vetrano, S., 2015. Mesenchymal stem cells reduce colitis in mice via release of TSG6, independently of their localization to the intestine. Gastroenterology 149, 163–176. http://dx.doi.org/10.1053/j.gastro.2015.03.013. (e20).

Santos, J.M., Camões, S.P., Filipe, E., Cipriano, M., Barcia, R.N., Filipe, M., Teixeira, M., Simões, S., Gaspar, M., Mosqueira, D., Nascimento, D.S., Pinto-do-Ó, P., Cruz, P., Cruz, H., Castro, M., Miranda, J.P., 2015. Three-dimensional spheroid cell culture of umbilical cord tissue-derived mesenchymal stromal cells leads to enhanced paracrine induction of wound healing. Stem Cell Res. Ther. 6. http://dx.doi.org/10.1186/s13287-015-0082-5.

Schafer, M., Werner, S., 2008. Oxidative stress in normal and impaired wound repair. Pharmacol. Res. 58, 165–171. http://dx.doi.org/10.1016/j.phrs.2008.06.004.

Sen, A., Kallos, M.S., Behie, L.A., 2001. Effects of hydrodynamics on cultures of mammalian neural stem cell aggregates in suspension bioreactors. Ind. Eng. Chem. Res. 40, 5350–5357. http://dx.doi.org/10.1021/ie001107y.

Song, H., Cha, M.-J., Song, B.-W., Kim, I.-K., Chang, W., Lim, S., Choi, E.J., Ham, O., Lee, S.-Y., Chung, N., Jang, Y., Hwang, K.-C., 2010. Reactive oxygen species inhibit adhesion of mesenchymal stem cells implanted into ischemic myocardium via interference of focal adhesion complex. Stem Cells 555–563. http://dx.doi.org/10.1002/stem.302.

Strand, B.L., Gåserød, O., Kulseng, B., Espevik, T., Skjåk-Bræk, G., 2002. Alginate-polylysine-alginate microcapsules: effect of size reduction on capsule properties. J. Microencapsul. 19, 615–630. http://dx.doi.org/10.1080/02652040210144243.

Tandara, A.A., Mustoe, T.A., 2004. Oxygen in wound healing − more than a nutrient. World J. Surg. 28, 294–300. http://dx.doi.org/10.1007/s00268-003-7400-2.

Tsai, A.-C., Liu, Y., Yuan, X., Ma, T., 2015. Compaction, fusion, and functional activation of three-dimensional human mesenchymal stem cell aggregate. Tissue Eng. Part A 21, 1705–1719.

Ungrin, M.D., Joshi, C., Nica, A., Bauwens, C., Zandstra, P.W., 2008. Reproducible, ultra high-throughput formation of multicellular organization from single cell suspension-Derived human embryonic stem cell aggregates. PLoS One 3, e1565. http://dx.doi.org/10.1371/journal.pone.0001565.

Wang, Y., Huang, L., Abdelrahim, M., Cai, Q., Truong, A., Bick, R., Poindexter, B., Sheikh-Hamad, D., 2009. Stanniocalcin-1 suppresses superoxide generation in macrophages through induction of mitochondrial UCP2. J. Leukoc. Biol. 86, 981–988. http://dx.doi.org/10.1189/jlb.0708454.

Wong, V.W., Rustad, K.C., Glotzbach, J.P., Sorkin, M., Inayathullah, M., Major, M.R., Longaker, M.T., Rajadas, J., Gurtner, G.C., 2011. Pullulan hydrogels improve mesenchymal stem cell delivery into high-oxidative-stress wounds. Macromol. Biosci. 1458–1466. http://dx.doi.org/10.1002/mabi.201100180.

Wu, J., Rostami, M.R., Cadavid Olaya, D.P., Tzanakakis, E.S., 2014. Oxygen transport and stem cell aggregation in stirred-suspension bioreactor cultures. PLoS One 9, e102486. http://dx.doi.org/10.1371/journal.pone.0102486.

Yagi, H., Soto-Gutierrez, A., Kitagawa, Y., Tilles, A.W., Tompkins, R.G., Yarmush, M.L., 2010. Bone marrow mesenchymal stromal cells attenuate organ injury induced by LPS and burn. Cell Transplant. 19, 823–830. http://dx.doi.org/10.3727/096368910x508942.

YlÖstalo, J.H., Bartosh, T.J., Coble, K., Prockop, D.J., 2012. Human mesenchymal Stem/stromal cells cultured as spheroids are self-activated to produce prostaglandin E2 that directs stimulated macrophages into an anti-inflammatory phenotype: hMSC spheroids promote M2 macrophage phenotype. Stem Cells 30, 2283–2296. http://dx.doi.org/10.1002/stem.1191.

Zanoni, M., Piccinini, F., Arienti, C., Zamagni, A., Santi, S., Polico, R., Bevilacqua, A., Tesei, A., 2016. 3D tumor spheroid models for in vitro therapeutic screening: a systematic approach to enhance the biological relevance of data obtained. Sci. Rep. 6, 19103. http://dx.doi.org/10.1038/srep19103.

Zhang, Q., Nguyen, A.L., Shi, S., Hill, C., Wilder-Smith, P., Krasieva, T.B., Le, A.D., 2012. Three-dimensional spheroid culture of human gingiva-derived mesenchymal stem cells enhances mitigation of chemotherapy-induced oral mucositis. Stem Cells Dev. 21, 937–947. http://dx.doi.org/10.1089/scd.2011.0252.

Zhao, G., Liu, F., Lan, S., Li, P., Wang, L., Kou, J., Qi, X., Fan, R., Hao, D., Wu, C., Bai, T., Li, Y., Liu, J.Y., 2015a. Large-scale expansion of Wharton's jelly-derived mesenchymal stem cells on gelatin microbeads, with retention of self-renewal and multipotency characteristics and the capacity for enhancing skin wound healing. Stem Cell Res. Ther. 6. http://dx.doi.org/10.1186/s13287-015-0031-3.

Zhao, X., Qiu, X., Zhang, Y., Zhang, S., Gu, X., Guo, H., 2015b. Three-dimensional aggregates enhance the therapeutic effects of adipose mesenchymal stem cells for ischemia-reperfusion induced kidney injury in rats. Stem Cells Int.

Zimmermann, J.A., Mcdevitt, T.C., 2014. Pre-conditioning mesenchymal stromal cell spheroids for immunomodulatory paracrine factor secretion. Cytotherapy 16, 331–345. http://dx.doi.org/10.1016/j.jcyt.2013.09.004.

dos Santos, F., Andrade, P.Z., Boura, J.S., Abecasis, M.M., da Silva, C.L., Cabral, J., 2010. Ex vivo expansion of human mesenchymal stem cells: a more effective cell proliferation kinetics and metabolism under hypoxia. J. Cell. Physiol. 223, 27–35.